

tal cancers. The confinement of the gene to a small amplicon in a subset of these tumors provides important, complementary evidence for the role of this gene in metastasis; the major genes previously shown to be amplified in naturally occurring cancers are all oncogenes (18, 23, 24). Extra copies of chromosome 8q DNA sequences have been observed in the advanced stages of many different tumor types, including advanced colon cancers (25–28). It has been suggested that the *c-MYC* gene on chromosome 8q24.12 is the target of such 8q overrepresentation. In the three metastatic lesions we examined, *c-MYC* was not amplified and was in fact located ~14 Mb from the boundaries of the *PRL-3* amplicon. It will, therefore, be of interest to evaluate the expression and genomic representation of *PRL-3* in the metastases of other cancer types.

Further experiments will be required to determine the biochemical mechanisms through which *PRL-3* influences neoplastic growth and to establish its causative role in the metastatic process. However, one of the most important ramifications of the work described here concerns its potential therapeutic implications. Most of the previously described genetic alterations in colorectal cancers involve inactivation of tumor suppressor genes. The proteins produced from these genes are difficult to target with drugs, because they are inactive or absent in the cancer cells (29). In contrast, enzymes whose expression is elevated in cancer cells, like that encoded by *PRL-3*, provide excellent targets for drug discovery purposes.

References and Notes

1. L. Weiss, *Cancer Metastasis Rev.* **19**, 193 (2000).
2. I. J. Fidler, *Surg. Oncol. Clin. N. Am.* **10**, 257, vii (2001).
3. A. Ridley, *Nature* **406**, 466 (2000).
4. K. W. Kinzler, B. Vogelstein, *Cell* **87**, 159 (1996).
5. V. E. Velculescu, B. Vogelstein, K. W. Kinzler, *Trends Genet.* **16**, 423 (2000).
6. SAGE libraries were generated with MicroSAGE, as described in a protocol available at [www.sagenet.org/sage\\_protocol.htm](http://www.sagenet.org/sage_protocol.htm). Reagents for this procedure were obtained from the I-SAGE kit available from Invitrogen (Carlsbad, California).
7. Examples of the nonepithelial transcripts identified in the initial libraries are vitronectin and lysozyme. These genes are transcribed in stromal cells and accounted for 0.4 and 0.1%, respectively, of the tags in SAGE libraries prepared from unpurified metastatic lesions but were not found in the SAGE library derived from purified metastatic epithelial cells. Similarly, transcripts made in hepatocytes, like apolipoprotein C-III, accounted for 0.3% of the tags from unpurified metastasis libraries but were not found in the libraries from purified cells. These differences in vitronectin, lysozyme, and apolipoprotein C-III expression among SAGE libraries derived from purified and unpurified epithelial cells were statistically significant ( $P < 0.0001$ ,  $\chi^2$  test).
8. Methods used in this study, including those used for purification of epithelial cells, are described in the supplementary Web material available on Science Online at [www.sciencemag.org/cgi/content/full/1065817/DC1](http://www.sciencemag.org/cgi/content/full/1065817/DC1).
9. V. E. Velculescu et al., *Nature Genet.* **23**, 387 (1999).
10. The metastasis-derived library was compared with two primary colorectal cancer and two normal colo-

rectal epithelial libraries (30). Monte Carlo simulations were used to identify transcripts that were expressed in the metastasis library at levels 10-fold higher or 10-fold lower than in the other libraries, with  $P$ -chance  $< 0.0001$ , as described (31). A complete listing of the SAGE tags and corresponding transcripts identified in this study is available at [www.sagenet.org](http://www.sagenet.org).

11. The transcripts chosen for further analysis included those for which the SAGE data indicated at least 10-fold greater expression in metastatic versus nonmetastatic lesions or for which the predicted gene products had potentially interesting functional properties.
12. Q. Zeng et al., *J. Biol. Chem.* **275**, 21444 (2000).
13. W. F. Matter et al., *Biochem. Biophys. Res. Commun.* **283**, 1061 (2001).
14. R. H. Diamond, D. E. Cressman, T. M. Laz, C. S. Abrams, R. Taub, *Mol. Cell. Biol.* **14**, 3752 (1994).
15. C. A. Cates et al., *Cancer Lett.* **110**, 49 (1996).
16. C. M. Perou et al., *Nature* **406**, 747 (2000).
17. D. Haber, E. Harlow, *Nature Genet.* **16**, 320 (1997).
18. G. M. Brodeur, M. D. Hogarty, in *The Genetic Basis of Human Cancer*, K. W. Kinzler, B. Vogelstein, Eds. (McGraw-Hill, New York, 1998), vol. 1, pp. 161–179.
19. The mouse homolog of *PRL-3* was mapped to a region of mouse chromosome 15 [23135.11cR on chromosome 15 in the radiation hybrid map of the Whitehead Institute Map (cR3000)] that is syntenic to the human 8q22–8q24.3 ([www.ncbi.nlm.nih.gov/Homology/view.cgi?chr=15&tax\\_id=10090](http://www.ncbi.nlm.nih.gov/Homology/view.cgi?chr=15&tax_id=10090)). STS (sequence tagged site) primers from the *PRL-3* gene and surrounding marker 145.8 (Fig. 3) were mapped to the Stanford G3 radiation hybrid panel. Both were shown to be tightly linked to marker SHGC-22154, located at 8q24.3, ~3 Mb from the 8q telomere. In comparison, *c-Myc* was mapped to 8q24.12–q24.13 in the Stanford G3 map, ~17 Mb from the telomere.
20. J. C. Venter et al., *Science* **291**, 1304 (2001).
21. E. S. Lander et al., *Nature* **409**, 860 (2001).
22. The *PRL-3* transcript (GenBank accession number NM\_032611) could not be identified in the Human Genome Project draft genome sequences, using standard tools including BLAST searches against the draft

genome sequence ([www.ncbi.nlm.nih.gov/genome/seq/page.cgi?F=HsBlast.html&&ORG=Hs](http://www.ncbi.nlm.nih.gov/genome/seq/page.cgi?F=HsBlast.html&&ORG=Hs)) and BLAT analyses of the assembled draft sequences (<http://genome.ucsc.edu/cgi-bin/hgBlat?command=start>). However, the *PRL-3* transcript was identical to Celera transcript hCT11716 and was found on Celera scaffold GA\_x2KMHMRCHQ1, CHGD Assembly Release 25h ([www.celera.com](http://www.celera.com)).

23. M. A. Heiskanen et al., *Cancer Res.* **60**, 799 (2000).
24. M. D. Pegram, G. Konecny, D. J. Slamon, *Cancer Treat. Res.* **103**, 57 (2000).
25. J. C. Alers et al., *Lab Invest.* **77**, 437 (1997).
26. A. Paredes-Zaglul et al., *Clin. Cancer Res.* **4**, 879 (1998).
27. N. N. Nupponen, J. Isola, T. Visakorpi, *Genes Chromosomes Cancer* **28**, 203 (2000).
28. A. El Gedaïly et al., *Prostate* **46**, 184 (2001).
29. B. Vogelstein, D. Lane, A. J. Levine, *Nature* **408**, 307 (2000).
30. L. Zhang et al., *Science* **276**, 1268 (1997).
31. V. E. Velculescu, L. Zhang, B. Vogelstein, K. W. Kinzler, *Science* **270**, 484 (1995).
32. Supported by the National Colorectal Cancer Research Alliance and NIH grants CA57345, CA 62924, and CA43460. K.W.K. received research funding from Genzyme Molecular Oncology (Genzyme). Under a licensing agreement between the Johns Hopkins University and Genzyme, the SAGE technology was licensed to Genzyme for commercial purposes, and B.V., K.W.K., and V.E.V. are entitled to a share of the royalties received by the university from the sales of the licensed technology. B.V., K.W.K., B.S.C., and V.E.V. are consultants to Genzyme. The university and researchers (B.V., K.W.K., V.E.V.) own Genzyme stock, which is subject to certain restrictions under university policy. The terms of these arrangements are being managed by the university in accordance with its conflict-of-interest policies. The SAGE technology is freely available to academia for research purposes.

29 August 2001; accepted 26 September 2001  
 Published online 11 October 2001;  
 10.1126/science.1065817  
 Include this information when citing this paper.

# Kinetic Stabilization of the $\alpha$ -Synuclein Protofibril by a Dopamine- $\alpha$ -Synuclein Adduct

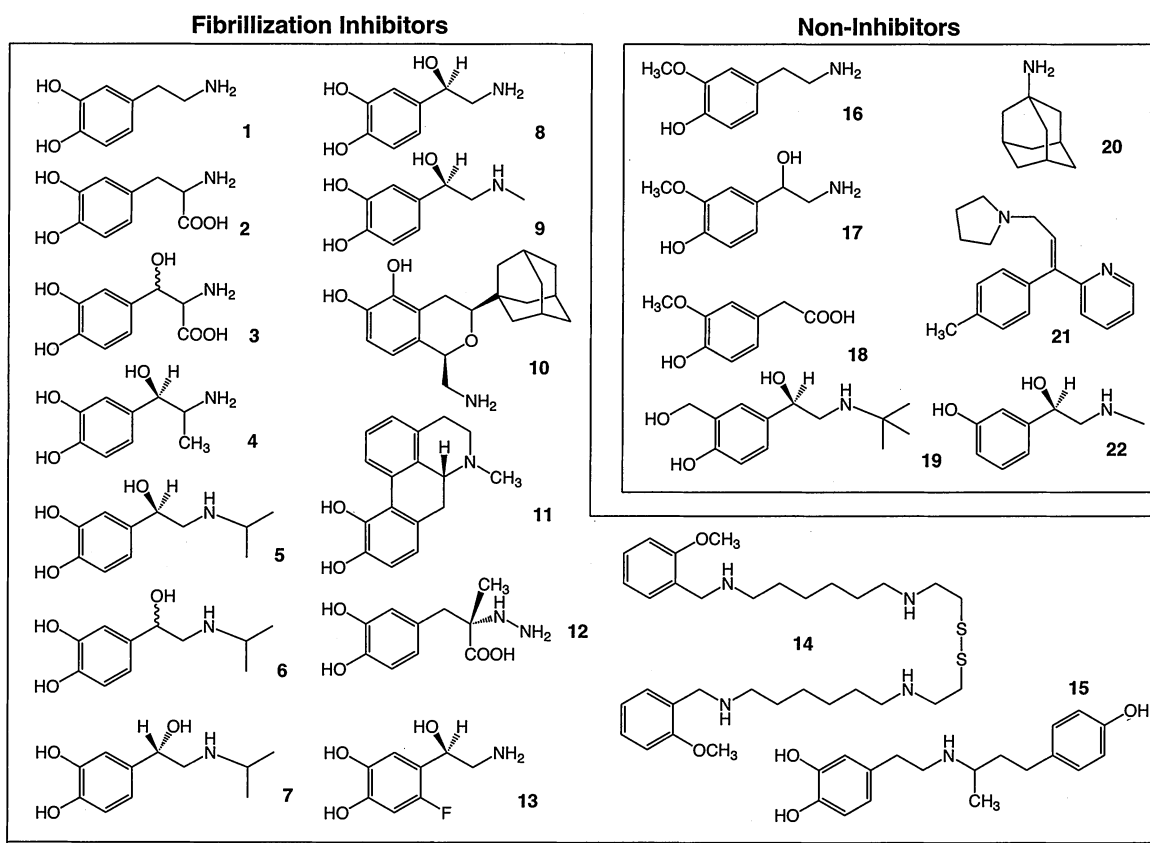
Kelly A. Conway,\* Jean-Christophe Rochet,\* Robert M. Bieganski, Peter T. Lansbury Jr.†

The substantia nigra in Parkinson's disease (PD) is depleted of dopaminergic neurons and contains fibrillar Lewy bodies comprising primarily  $\alpha$ -synuclein. We screened a library to identify drug-like molecules to probe the relation between neurodegeneration and  $\alpha$ -synuclein fibrilization. All but one of 15 fibril inhibitors were catecholamines related to dopamine. The inhibitory activity of dopamine depended on its oxidative ligation to  $\alpha$ -synuclein and was selective for the protofibril-to-fibril conversion, causing accumulation of the  $\alpha$ -synuclein protofibril. Adduct formation provides an explanation for the dopaminergic selectivity of  $\alpha$ -synuclein-associated neurotoxicity in PD and has implications for current and future PD therapeutic and diagnostic strategies.

A central role for  $\alpha$ -synuclein fibrilization in PD (1, 2) is supported by the fact that fibrillar  $\alpha$ -synuclein is a major component of Lewy bodies (3, 4) and that the  $\alpha$ -synuclein gene has been linked to autosomal dominant PD (FPD) (5, 6). Although both FPD  $\alpha$ -synuclein mutations [Ala<sup>53</sup> → Thr (A53T) and Ala<sup>30</sup> → Pro (A30P)] accelerate the formation of nonfibrillar,

oligomeric protofibrils in vitro, A30P inhibits the conversion of protofibrils to fibrils (7). This finding suggests that protofibrils may be pathogenic and fibrils inert, or even protective (2). Transgenic mice that express wild-type human  $\alpha$ -synuclein (8) exhibit PD-like dopaminergic deficits and motor dysfunction, and they develop neuronal inclusions that, in contrast to those

**Fig. 1.** Catechol-containing compounds inhibit  $\alpha$ -synuclein fibrillization. Structures of 22 out of 169 compounds (assayed at 100 to 300  $\mu$ M) from our initial screening library divided according to their activity in an in vitro thioflavin T (Thio T) assay (7). A53T  $\alpha$ -synuclein (175 to 300  $\mu$ M) was used in initial screens, but inhibition was confirmed with the wild type. Incubations were done with shaking (reading at 1 day) or without (reading at 30 days) at 37°C. Inhibitors decreased the Thio T signal by  $\geq 50\%$  in all four trials. This screen was not designed to precisely measure inhibitory activity. One out of 155 non-catechol compounds screened, **14**, met the above criteria. The requirement for a catechol ring was reinforced by the inactivity of compounds **16**, **17**, **18**, **19**, and **22**.



of the Parkinsonian humans and *Drosophila* (9), are entirely nonfibrillar. Crossing these mice with a second transgenic line expressing  $\beta$ -synuclein produces mice in which the number of nonfibrillar inclusions and the Parkinsonian phenotype are reduced, which suggests that protofibrils may cause disease (10).

Drug-like molecules could be used in animal models to probe the relation between the conversion of  $\alpha$ -synuclein to protofibrils (and then to fibrils) and the progression of neuronal loss and motor dysfunction. If the protofibril is pathogenic, then delaying the appearance of fibrillar inclusions by stabilizing protofibrillar intermediates may accelerate the onset and progression of motor abnormalities (2). In contrast, inhibiting the formation of both protofibrils and fibrils could slow disease progression (10). To identify compounds that inhibit the formation of  $\alpha$ -synuclein amyloid fibrils (7), we screened a commercially available compound library (11). Fifteen of 169 compounds initially screened inhibited  $\alpha$ -synuclein fibrillization

Center for Neurologic Diseases, Brigham and Women's Hospital, Department of Neurology, Harvard Medical School, 65 Landsdowne Street, Cambridge, MA 02139, USA.

\*These authors contributed equally to this work.  
 †To whom correspondence should be addressed. E-mail: plansbury@rics.bwh.harvard.edu

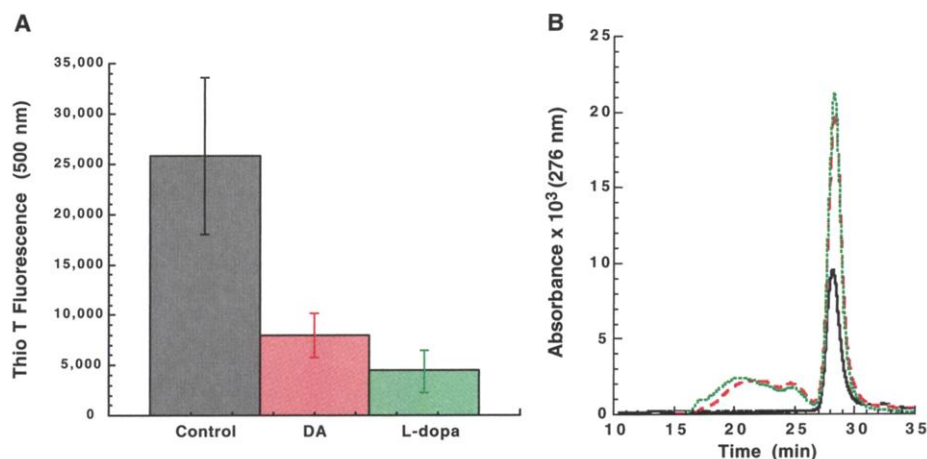


**Fig. 2.** Catecholamines inhibit  $\alpha$ -synuclein fibril formation, modify monomer, and stabilize UV-active oligomers; effects are eliminated by antioxidants. Samples of 180  $\mu$ M A53T  $\alpha$ -synuclein were incubated alone or with equimolar DA or L-dopa at 37°C with agitation. After 3 days, aliquots from each incubation were analyzed by Thio T to measure fibrils (A) and were subjected to gel filtration chromatography to measure nonfibrillar species (B). In (A), DA and L-dopa inhibit  $\alpha$ -synuclein fibril formation; the effect is reversed by the addition of 1% w/v  $\text{Na}_2\text{S}_2\text{O}_5$  (53 mM) or by 3 molar equivalents each of *N*-acetyl cysteine and desferoximine (36). In (B), DA (dashed red line) and L-dopa (dotted green line) stabilize the formation of oligomeric  $\alpha$ -synuclein (broad peak eluting between 17 and 27 min) and increase the UV activity of the monomer peak (28 min) as compared to time 0 (36). No protofibrils were detected in the control incubation (solid black line). Addition of 1% w/v  $\text{Na}_2\text{S}_2\text{O}_5$  eliminates the catechol-induced effects (36).

(Fig. 1). All but one of the inhibitors were catecholamines, including dopamine (DA) (1) and L-dopa (2), norepinephrine (8), and

epinephrine (9). The inhibitory activity of DA and L-dopa (Fig. 2A) was reversed by the addition of antioxidants, which suggested that

## REPORTS

catechol oxidation was responsible (11, 12).

Under inhibitory conditions, protofibrils accumulated (13) and the ultraviolet (UV) absorption of the residual monomeric  $\alpha$ -synuclein increased (Fig. 2B). Both phenomena were eliminated by sodium metabisulfite, suggesting that fibril inhibition, protofibril accumulation, and monomer modification may be consequences of covalent modification by the dopamine-derived orthoquinone [DAQ; see (11)]. Although  $\alpha$ -synuclein does not contain cysteine, which reacts with DAQ in vitro and in vivo (14), its natively unfolded structure (15) may expose other reactive side chains such as Tyr, Lys, or Met. The DA-modified  $\alpha$ -synuclein monomer produced a long-wavelength (468 nm) fluorescence emission, consistent with a Tyr-derived radical coupling adduct (Fig. 3A) (16). Because analysis by mass spectrometry suggested that adduct formation occurred at low levels (less than 10% of parent ion intensity was potentially due to adduct), the possible incorporation of radiolabeled DA was monitored. [ $^3\text{H}$ ]DA incorporation (DA concentration = 2 mM) into monomeric (Fig. 3B; Fig. 3D, left panel) and then protofibrillar (Fig. 3C; Fig. 3D, right panel)  $\alpha$ -synuclein occurred at a rate comparable to DA polymerization, a process that is known to occur in vivo (17, 18). After purification of the monomeric adduct, the average level of DA incorporation (moles of [ $^3\text{H}$ ]DA per mole of protein) was estimated to be 5 to 10% (Fig. 3E, blue bars). The monomeric adduct was stable to boiling (Fig. 3E, red bars) and stained [SDS-polyacrylamide gel electrophoresis (PAGE)] with a redox-active system that identifies catechol-containing proteins (19). Together, these data are consistent with the formation of low levels of one or more DA- $\alpha$ -synuclein covalent adducts, possibly derived from radical coupling (DAQ to Tyr) and/or nucleophilic attack (e.g., Lys forming a Schiff base with DAQ) (20, 21).

The partially modified  $\alpha$ -synuclein monomer was separated from protofibrillar material and from free DA, and its fibrilization in the absence of DA was compared to that of unmodified  $\alpha$ -synuclein monomer (Fig. 4, yellow versus black bars). In addition, parallel incubations in which the adduct was diluted with unmodified  $\alpha$ -synuclein (total  $\alpha$ -synuclein concentration was constant) were also followed (Fig. 4, red and green bars). Fibril formation (Fig. 4A) was fastest in the unmodified incubation, and the degree of inhibition was correlated to the concentration of adduct(s). Protofibrils were observed as transient intermediates in every incubation and were most long-lived in the incubations containing trace amounts of DA- $\alpha$ -synuclein adduct (Fig. 4B, green bars). This effect was observed even in the case where the DA adduct was diluted 1:4 and represented about 1 to 3% of the total  $\alpha$ -synuclein (Fig. 4B, red bars). Nucleation-dependent protein oligomerization processes can be inhibited by

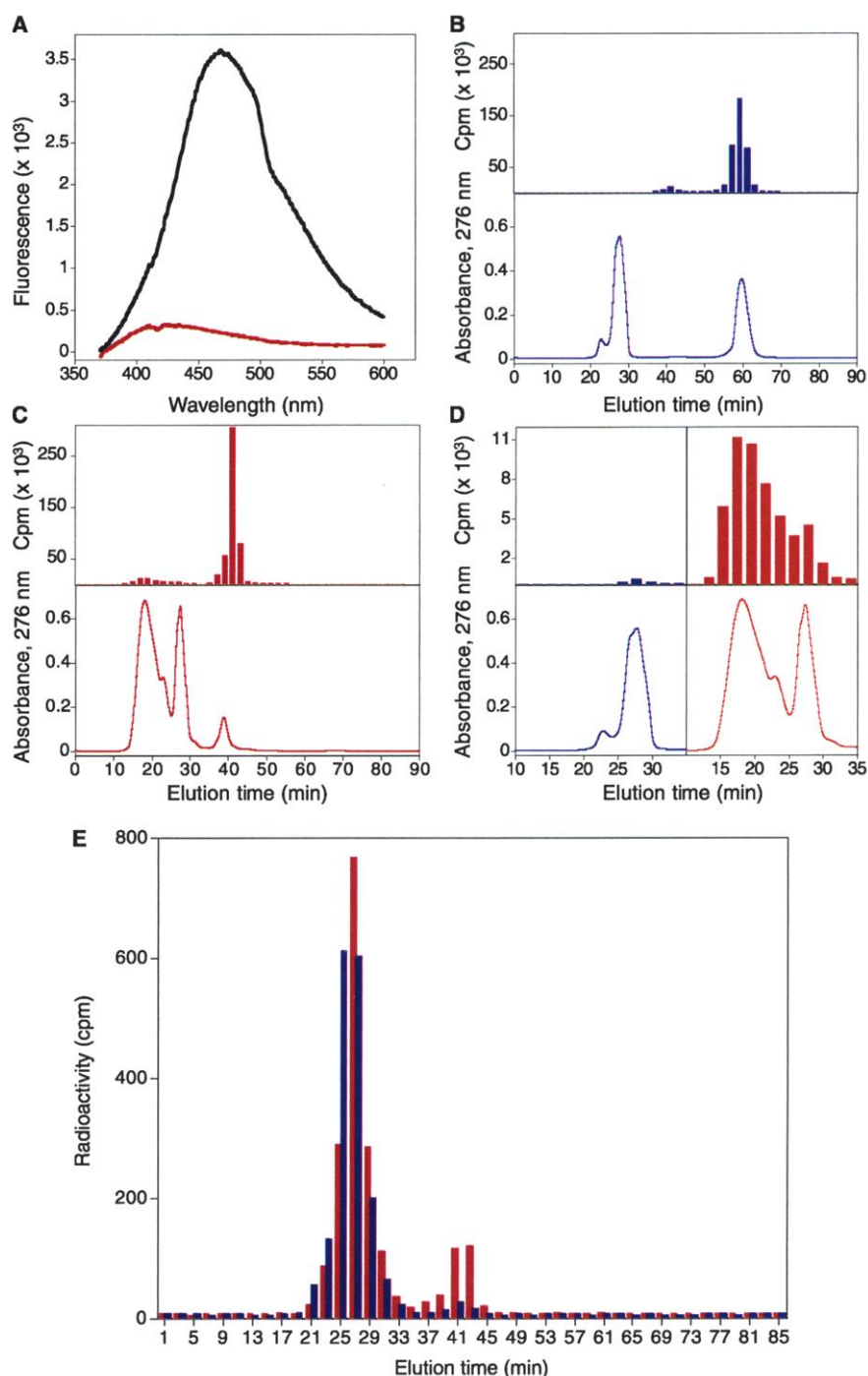


**Fig. 3.** DAQ reacts with  $\alpha$ -synuclein to form fluorescent covalent adducts. (A) Fluorescence emission spectra of monomeric DA-treated A53T (8.9  $\mu\text{M}$ , black line) and untreated A53T (18  $\mu\text{M}$ , red line). Excitation wavelength, 360 nm; wavelength of maximal emission ( $\lambda_{\text{max}}$ ): DA-treated A53T, 468 nm; untreated A53T, 426 nm. (B to D) Gel filtration of a solution of A53T (1 mM) treated with [ $^3\text{H}$ ]DA (2 mM, 5 mCi/mmol), monitored by scintillation counting (top) and absorbance at 276 nm (bottom). The solution was analyzed immediately (B) or after incubation for 11 days at 37°C without rotation (C). The left and right panels of (D) correspond to data from (B) and (C), respectively, showing the elution of oligomeric and monomeric  $\alpha$ -synuclein between 10 and 35 min (DA elutes at 60 min, and its oxidative polymerization product, which is also formed in the absence of  $\alpha$ -synuclein, elutes at 39 min). (E) Gel-purified monomer [from (C)] was analyzed before (blue bars) and after (red bars) boiling for 10 min.

trace impurities, which act like crystal poisons (22). This effect, which may explain the results above, has been demonstrated in the case of  $\alpha$ -synuclein fibrilization, where a small relative

amount of human  $\alpha$ -synuclein inhibits fibrilization of its mouse homolog (13).

Cell death in PD largely affects the substantia nigra. The selective loss of dopaminergic

REPORTS

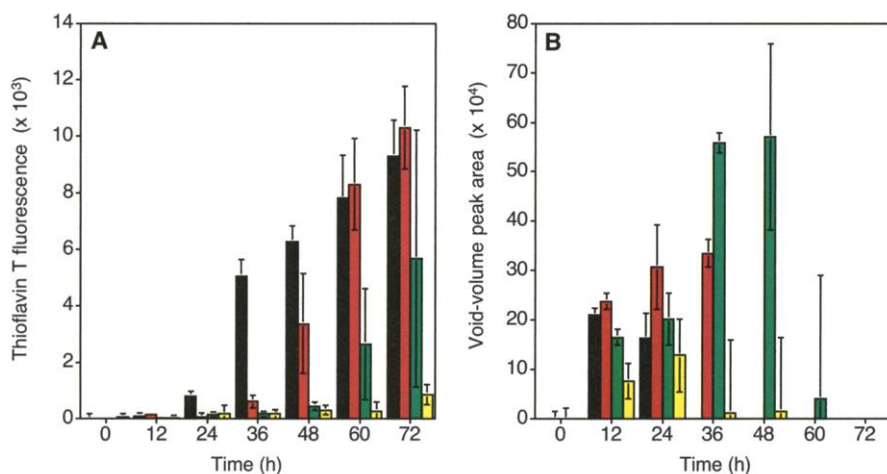


**Fig. 4.** Monomeric DA- $\alpha$ -synuclein adduct inhibits  $\alpha$ -synuclein fibrilization but prolongs the lifetime of the protofibrillar intermediates. Incubations containing unmodified wild type (600  $\mu$ M, black bars), DA-modified wild type (600  $\mu$ M, yellow bars), or mixtures of the unmodified and modified proteins [450  $\mu$ M unmodified + 150  $\mu$ M modified (red bars); 300  $\mu$ M unmodified + 300  $\mu$ M modified (green bars)] were rotated at 37°C and analyzed at various times. (A) The Thio T assay shows that fibril formation is fastest in unmodified incubation and slowest in the incubation containing the highest level of DA adduct. (B) Void-volume (protofibril) peak area determined by gel filtration and UV (absorbance at 215 nm). At time points where no protofibril was detected (e.g., 72 hours), the bar was omitted. Absorbance attributed to a small amount of oligomeric material present in the unmodified sample at time 0, as a result of freeze-thawing, was subtracted from subsequent measurements. Protofibrils were most persistent at trace levels of adduct (green bars), but their formation is inhibited at a higher level of modification (yellow bars), indicating that high levels of adduct also inhibit the monomer-to- protofibril transition.

neurons is mimicked whether Parkinsonism is induced in *Drosophila* by brain-wide expression of  $\alpha$ -synuclein (9) or in rats by chronic systemic exposure to rotenone, a complex I inhibitor (23). Thus, three established risk factors—oxidative stress, DA, and  $\alpha$ -synuclein—may, in combination, stabilize protofibrillar  $\alpha$ -synuclein and promote the pathogenesis of PD (1, 11). As a prerequisite,  $\alpha$ -synuclein levels must exceed the critical concentration for oligomerization. In rare familial forms of PD, that threshold may be lowered by  $\alpha$ -synuclein point mutations (7). In other forms of PD, elevated levels of wild-type  $\alpha$ -synuclein could result from its inefficient degradation due to PD-associated parkin mutations (24, 25) or its overexpression due to PD-associated promoter polymorphisms (26, 27). The  $\alpha$ -synuclein message is up-regulated in PD substantia nigra, but not in cerebellum or cortex (28). Once the critical concentration of  $\alpha$ -synuclein has been exceeded, the cytoplasmic concentration of DAQ may be one of several factors that determine the amount and lifetime of potentially pathogenic  $\alpha$ -synuclein protofibrils. DAQ results from a combination of oxidative stress and elevated cytoplasmic DA concentration, both of which are independently associated with PD (14). The importance of cytoplasmic DA in PD cell death is supported by two facts: (i) The dopaminergic neurons of the ventral tegmental area—which are resistant relative to the substantia nigra—express high levels of VMAT2, which promotes vesicular sequestration of DA, and low levels of DAT, which pumps DA into the cytoplasm (29); and

(ii) neurons containing neuromelanin, a polymerization product of DAQ, are relatively sensitive to PD-induced cell death (18). Differences in transport and vesicular packaging may also explain why the noradrenergic system is relatively spared in PD, even though epinephrine and norepinephrine are oxidatively labile and capable of adduct formation. DA and some of its analogs are neurotoxic in cell culture (30), and this effect has been linked to  $\alpha$ -synuclein (31). A distinct but overlapping combination of factors may contribute to the pathogenesis of diffuse Lewy body disease (DLBD), a dementia that is characterized by  $\alpha$ -synuclein inclusions and degeneration of the cortex. Thus, high cortical expression of  $\alpha$ -synuclein [mRNA level is elevated in DLBD (28)] may combine with other trace  $\alpha$ -synuclein modifications (32) to stabilize protofibrils.

Decreasing  $\alpha$ -synuclein expression and preventing protofibril accumulation are two attractive therapeutic strategies against PD. The latter could be accomplished by decreasing the cytoplasmic concentration of DA, an endogenous protofibril stabilizer, while avoiding depletion of synaptic DA, which ameliorates PD symptoms. Although there is no consistent evidence regarding a potentially neurotoxic effect of L-dopa therapy that is suggested by this work (33), clinical trials to address this issue are in progress (34).

References and Notes

1. T. M. Dawson, *Cell* **101**, 115 (2000).
2. M. S. Goldberg, P. T. Lansbury Jr., *Nature Cell Biol.* **2**, E115 (2000).

3. M. G. Spillantini et al., *Nature* **388**, 839 (1997).
4. M. Baba et al., *Am. J. Pathol.* **152**, 879 (1998).
5. R. Kruger et al., *Nature Genet.* **18**, 106 (1998).
6. M. H. Polymeropoulos et al., *Science* **276**, 2045 (1997).
7. K. A. Conway et al., *Proc. Natl. Acad. Sci. U.S.A.* **97**, 571 (2000).
8. E. Masliah et al., *Science* **287**, 1265 (2000).
9. M. B. Feany, W. W. Bender, *Nature* **404**, 394 (2000).
10. M. Hashimoto et al., *Neuron* **32**, 213 (2001).
11. See supplemental material at Science Online ([www.sciencemag.org/cgi/content/full/294/5545/1346/DC1](http://www.sciencemag.org/cgi/content/full/294/5545/1346/DC1)).
12. In the absence of DA, oxidative conditions (e.g., hydrogen peroxide) were not inhibitory.
13. J. C. Rochet, K. A. Conway, P. T. Lansbury Jr., *Biochemistry* **39**, 10619 (2000).
14. S. B. Dunnett, A. Bjorklund, *Nature* **399** (suppl.), A32 (1999).
15. P. H. Weinreb et al., *Biochemistry* **35**, 13709 (1996).
16. Intramolecular dityrosine formation was ruled out by the fluorescence emission maximum, the failure to observe dityrosine after hydrolysis, and the failure to detect the modified monomer by Western blot using a monoclonal antibody that detects dityrosine-containing proteins (35).
17. SDS-PAGE analysis of oligomeric  $\alpha$ -synuclein (Fig. 2B) revealed a ladder of SDS-stable oligomers, presumably cross-linked species. These species had no effect on  $\alpha$ -synuclein fibrilization.
18. D. Sulzer et al., *Proc. Natl. Acad. Sci. U.S.A.* **97**, 11869 (2000).
19. D. M. Kuhn, R. Arthur, *J. Neurosci.* **18**, 7111 (1998).
20. L. A. Burzio, J. H. Waite, *Biochemistry* **39**, 11147 (2000).
21. None of the 10  $\alpha$ -synuclein antibodies available to us are able to immunoprecipitate the adduct(s). Four of the 10 [7071 (rabbit polyclonal; ours), LB509 (mouse monoclonal; Zymed), AB116-131] (goat polyclonal; Research Diagnostics), and syn-1 (mouse monoclonal; Transduction Laboratories)] selectively precipitated the unmodified protein, enriching the remaining soluble protein for the radiolabeled adduct. This result suggests that the relevant epitopes were modified, either covalently or conformationally, by adduct formation. The six other antibodies [AB5038 (rabbit polyclonal; Chemicon), AB2-25] (rabbit polyclonal; Synaptic Systems), sc-7011 (goat polyclonal; Santa Cruz), sc-7012 (goat polyclonal; Santa Cruz), AB5336P (sheep polyclonal; Chemicon), and AB5334P (sheep polyclonal; Chemicon)] did not immunoprecipitate the adduct or the unmodified protein.
22. J. T. Jarrett, P. T. Lansbury Jr., *Cell* **73**, 1055 (1993).
23. R. Betarbet et al., *Nature Neurosci.* **3**, 1301 (2000).
24. H. Shimura et al., *Science* **293**, 263 (2001).
25. M. Farrer et al., *Ann. Neurol.* **50**, 1 (2001).
26. J. W. Touchman et al., *Genome Res.* **11**, 78 (2001).
27. M. Farrer et al., *Hum. Mol. Genet.* **10**, 1 (2001).
28. E. Rockenstein et al., *Brain Res.* **914**, 48 (2001).
29. N. Takahashi et al., *Proc. Natl. Acad. Sci. U.S.A.* **94**, 9938 (1997).
30. T. G. Hastings, D. A. Lewis, M. J. Zigmond, *Proc. Natl. Acad. Sci. U.S.A.* **93**, 1956 (1996).
31. S. J. Tabrizi et al., *Hum. Mol. Genet.* **9**, 2683 (2000).
32. B. I. Giasson et al., *Science* **290**, 985 (2000).
33. Y. Agid, *Neurology* **50**, 858 (1998).
34. S. Fahn, *Arch. Neurol.* **56**, 529 (1999).
35. Y. Kato et al., *Biochem. Biophys. Res. Commun.* **275**, 11 (2000).
36. K. A. Conway, J.-C. Rochet, R. M. Bieganski, P. T. Lansbury Jr., data not shown.
37. We thank M. Schlossmacher, M. Feany, M. LaVoie, and D. Selkoe for reading this manuscript and providing helpful comments. We also thank J. Hardy and E. Masliah for sharing their unpublished results, cited here. Supported by a Morris K. Udall Parkinson's Disease Research Center of Excellence grant (NS38375) and the James K. Warsaw Foundation to Cure Parkinson's Disease. J.-C.R. is postdoctoral fellow of the Human Frontiers Science Program and the Alberta Heritage Foundation for Medical Research.

18 June 2001; accepted 24 September 2001